

Accepted Manuscript

A highly sensitive luminescent probe based on Ru(II)-bipyridine complex for Cu²⁺, l-histidine detection and cellular imaging

Shi-Ting Zhang, Panpan Li, Caiyun Liao, Tingting Luo, Xingming Kou, Dan Xiao



PII: S1386-1425(18)30391-3
DOI: doi:[10.1016/j.saa.2018.05.001](https://doi.org/10.1016/j.saa.2018.05.001)
Reference: SAA 16024

To appear in: *Spectrochimica Acta Part A: Molecular and Biomolecular Spectroscopy*

Received date: 16 August 2017
Revised date: 29 April 2018
Accepted date: 1 May 2018

Please cite this article as: Shi-Ting Zhang, Panpan Li, Caiyun Liao, Tingting Luo, Xingming Kou, Dan Xiao , A highly sensitive luminescent probe based on Ru(II)-bipyridine complex for Cu²⁺, l-histidine detection and cellular imaging. The address for the corresponding author was captured as affiliation for all authors. Please check if appropriate. Saa(2017), doi:[10.1016/j.saa.2018.05.001](https://doi.org/10.1016/j.saa.2018.05.001)

This is a PDF file of an unedited manuscript that has been accepted for publication. As a service to our customers we are providing this early version of the manuscript. The manuscript will undergo copyediting, typesetting, and review of the resulting proof before it is published in its final form. Please note that during the production process errors may be discovered which could affect the content, and all legal disclaimers that apply to the journal pertain.

A highly sensitive luminescent probe based on Ru(II)-bipyridine complex for Cu²⁺, L-Histidine detection and cellular imaging

Shi-Ting Zhang^a, Panpan Li^b, Caiyun Liao^a, Tingting Luo^a, Xingming Kou^{*,a}, Dan Xiao^{*,a,c}

^aCollege of Chemistry, Sichuan University, Chengdu 610064, China.

^bDepartment of Architecture and Environment, Sichuan University, Chengdu 610065, China

^cCollege of Chemical Engineering, Sichuan University, Chengdu 610065, China.

*Corresponding Author: Xingming Kou E-mail: kouxm@scu.edu.cn; Dan Xiao E-mail: xiaodan@scu.edu.cn.

Abstract

A ruthenium(II) bipyridyl complex conjugated with functionalized Schiff base (RuA) has been synthesized and functioned as a luminescent probe. The luminescence of RuA was greatly quenched by Cu^{2+} due to its molecular coordination with paramagnetic Cu^{2+} . Subsequently, the addition of L-Histidine can turn on the luminescence of the RuA-Cu(II) ensemble, which can be attributed to the replacement of RuA in RuA-Cu(II) ensemble by L-Histidine. On the basis of the quenching and recovery of the luminescence of RuA, we proposed a rapid and highly sensitive on-off-on luminescent assay for sensing Cu^{2+} and L-Histidine in aqueous solution. Under the optimal conditions, Cu^{2+} and L-Histidine can be detected in the concentration range of 5 nM–9.0 μM and 50 nM–30 μM , respectively, and the corresponding detection limits were calculated to be 0.35 and 0.44 nM (S/N=3), separately. The proposed luminescent probe has been successfully utilized for the analysis of Cu^{2+} and L-Histidine in real samples (drinking water and biological fluids). Furthermore, the probe revealed good photostability, low cytotoxicity and excellent permeability, making it a suitable candidate for cell imaging and labeling in vitro.

Keywords

Luminescent detection; Cu^{2+} ; L-Histidine; Ruthenium(II) complex; Cell imaging

1. Introduction

As an essential element of the organism, copper is the third largest essential trace element in the human body after iron and zinc [1,2]. Specially, Cu^{2+} plays a key role in signal transduction, cellular energy generation, together with oxygen transport and activation [3,4], because copper ions are the redox cofactor of many mitochondria, cytosol and vesicle oxidase coenzyme [5]. However, due to the uncontrolled reaction presented in Cu^{2+} with oxygen and reactive oxygen species (ROS), it may also cause oxidative damage to nucleic acids, proteins and lipids [6-9]. For example, some grievous neurodegenerative

diseases, such as Wilson, Menkes, prion and Alzheimer's disease, are associated with the change of homeostasis Cu^{2+} in intracellular [3,10-12].

In addition to the transition metal, we are also concerned about the physiological role of amino acids. L-Histidine (L-His) is involved in numerous key biological activities in the human body, including minimizing minimally invasive internal bleeding and controlling the transport of metals in vital genes [13,14]. For example, L-His, as an important neurotransmitter, is the metabolic disorder indicator of many diseases and psychological disorders, such as the failure of normal erythropoietin and Parkinson's, epilepsy disease, etc [15-18].

Therefore, the design and synthesis of probes for Cu^{2+} and L-His detection have attracted much attention. As one of the important methods for testing Cu^{2+} , luminescent probe displays much clear superiority in selectivity and biological imaging due to its sensitivity, specificity, easy operation and real-time detection with fast response [19-21]. As for L-His, luminiferous detection has received great attention for its temporal and spatial resolution and high sensitivity [22,23]. Some metal indicator complexes (called ensembles) have been considered as molecular luminescent probes for L-His [24-26].

In recent years, many probes have been reported for the detection of Cu^{2+} . However, many of them performed in acetonitrile, ethanol, methanol or other organic solvents [27-30] and required prolonged reaction time [31,32], which limits their practical applications especially in biological systems and further lead to lower detection efficiency. To the best of our knowledge, due to their satisfied water solubility, intense polarized luminescence, high chemical and optical stability, large Stokes shifts, relatively long lifetimes and low-energy absorption [33,34], ruthenium(II) polypyridyl complexes have turned into prospective probe for environmental monitoring and biological probing [35-38].

Therefore, in this work, we have designed a Ru(II) polypyridyl complex-based probe that can selectively detect Cu^{2+} , and then the probe-Cu(II) complex acted as an ensemble

to identify L-His. Specifically, the design strategy was based on the imino N and phenol O atoms of RuA (the abbreviation of $\text{Ru}(\text{bpy})_2(\text{A})\text{Cl}_2$, where $\text{bpy} = 2,2'$ -bipyridine, $\text{A} = \text{N},\text{N}'$ -5,6-(1,10-phenanthroline)-bis(5-methoxysalicylidene)diamine) can efficiently combine Cu^{2+} centre (d^9) resulting in the luminescence quenching [39-41]. In order to further validate the sensing mechanism, we synthesized a series of compounds (RuB, RuC and RuD) with the similar molecular structure and conducted comparative studies. Moreover, the luminescent intensity of RuA-Cu(II) can be obviously enhanced by adding L-His, which indicated that RuA-Cu(II) ensemble can be used as the luminescent probe for L-His detection. Besides, the obtained probe exhibited many favorable properties, such as red emission, 100% water solubility and biocompatibility, implying its potential to be used in the bio-detection in vivo and in vitro. Consequently, RuA showed a possibility to serve as an on-off-on luminescent switch probe to selectively, sensitively and quickly detect Cu^{2+} and L-His in aqueous solution and biological fluids. Furthermore, cell imaging experiments showed that RuA exhibited fine membrane permeability, very low toxicity, and the capability of visualizing Cu^{2+} and L-His in living cells.

2. Experimental Section

2.1. Materials

1,10-phenanthroline-5,6-diamine was synthesized and purified according to our previous literature [42]. 2-hydroxyl-5-methoxybenzaldehyde was purchased from Aladdin Industrial Corporation (Shanghai, China). Cis-Bis-(2,2'-bipyridine) dichlororuthenium(II) dihydrate ($\text{Ru}(\text{bpy})_2\text{Cl}_2 \cdot 2\text{H}_2\text{O}$, 99%) was gained from Alfa Aesar (Johnson Matthey Company, U.S.A.). Mice B16 melanoma cells were purchased from the Shanghai Institute of Biochemistry and Cell Biology, Chinese Academy of Sciences. Roswell Park Memorial Institute (RPMI)-1640 medium and fetal bovine serum (FBS) were obtained from Life Technologies Corporation (Gibco, USA). A Cell-Counting Kit-8 (CCK-8) was purchased from Dojindo Laboratories (Tokyo, Japan). Lyophilized human serum samples were purchased from Boer Xi Science and Technology (China) Co., Ltd. Other chemical

reagents and solvents were purchased from commercial chemical suppliers and used without further purification.

2.2. Apparatus

Fluorescence spectra (FL) were measured on a Hitachi F-7000 fluorescence spectrophotometer (Japan). UV-Vis absorption spectra were recorded on U-2900 spectrophotometer (HITACHI, Japan). ^1H NMR was measured on a Bruker AV II-400 MHz spectrometer. FT-IR was performed on a Thermo Scientific Nicolet 6700 FT-IR spectrometer (Sugar Land, TX, USA). Mass spectra of A was obtained from the MAT-261 spectrometer (Thermo Fisher Scientific, San Jose, CA). Matrix-assisted laser desorption/ionization time of flight mass spectrometry (MALDI-TOF-MS) of RuA was obtained from a Bruker Ultrafle Xtreme matrix-assisted laser desorption/ionization time of flight mass spectrometer (Germany). Fluorescence lifetime measurements were acquired using a Fluorolog-3 spectrofluorometer (Horiba Jobin Yvon) with a NanoLED (454 nm, Horiba Scientific) as the excitation source and a picosecond photon detection module (PPD-850, Horiba Scientific) as the detector. Confocal luminescence imaging was performed by a confocal laser scanning microscopy (Nikon, N-SIM).

2.3. Synthesis

N,N' -5,6-(1,10-phenanthroline)-bis(5-methoxyl-salicylidene)diamine (A), RuA, RuB, RuC and RuD were prepared by the following steps (Scheme 1, Scheme S1). Products were characterized by ^1H NMR, FT-IR, HRMS and elemental analysis (Fig. S15-23[†]).

2.3.1. Synthesis of A

A mixture of 1,10-phenanthroline-5,6-diamine (200 mg, 0.95 mmol) and 2-hydroxy-5-methoxybenzaldehyde (475 μL , 3.8 mmol) was dissolved in ethanol (20 mL) and a few drops of triethyl orthoformate were added. Then the mixture was stirred at 76 $^\circ\text{C}$ for 4 h under reflux in a nitrogen atmosphere. After cooling to room temperature, the product was obtained via filtration, washed with diethyl ether and dried under vacuum. Yield: 53.7%. ^1H NMR (400 MHz, DMSO-d_6) δ (ppm): δ 12.28 (s, 2H), 9.08 (s, 3H),

8.98–8.87 (m, 3H), 7.95–7.74 (m, 5H), 7.05 (s, 4H), 3.86 (s, 5H). FT-IR (KBr): 3430.36 cm^{-1} (OH), 1565.38 cm^{-1} (C=N imines), 1492.49 cm^{-1} (OCH₃), 1223.26 cm^{-1} and 1039.94 cm^{-1} (=C-O-C-), 737.22 cm^{-1} (benzene ring substitution). ESI-MS: calcd for C₂₈H₂₂O₄N₄ ([M+Na]⁺): 501.502, found: 501.155. Elemental analysis: calcd (%) for C₂₈H₂₂O₄N₄ (478.512): C 70.28, H 4.63, N 11.71; found: C 69.55, H 4.92, N 12.25.

2.3.2. Synthesis of RuA

Ru(bpy)₂C₂·2H₂O (30 mg, 0.057 mmol) and A (27.3 mg, 0.057 mmol) were dissolved in dry ethanol (15 mL) under nitrogen. The solution was refluxed at 80 °C for 12 h under nitrogen atmosphere. Then the deep red solution was cooled and the solvent was removed by vacuum distillation. The crude residue was purified by column chromatography (SiO₂, CH₂Cl₂/CH₃OH 4:1, v/v) and a red solid was obtained. Yield: 79.4%. ¹H NMR (400 MHz, DMSO-d₆) δ (ppm): δ 8.90 (dd, *J* = 15.4, 8.2 Hz, 6H), 8.23 (td, *J* = 8.0, 1.3 Hz, 3H), 8.11 (td, *J* = 8.0, 1.3 Hz, 3H), 8.02 (d, *J* = 4.7 Hz, 3H), 7.92–7.83 (m, 5H), 7.67–7.56 (m, 5H), 7.40–7.33 (m, 3H), 7.19–7.12 (m, 1H), 6.98 (s, 2H), 6.76 (d, *J* = 7.5 Hz, 1H), 3.87 (s, 4H). FT-IR (KBr): 3392.67 cm^{-1} (OH), 1598.59 cm^{-1} (C=N imines), 1439.10 cm^{-1} (OCH₃), 1239.25 cm^{-1} and 1028.71 cm^{-1} (=C-O-C-), 764.50 cm^{-1} (benzene ring substitution). ESI-MS: calcd for C₄₈H₃₈O₄N₈RuCl₂ ([M-2Cl+H]³⁺): 890.950, found: 890.938. ([M-Cl+Na+2H]²⁺): 952.417, found: 952.895. Elemental analysis: calcd (%) for C₄₈H₃₈O₄N₈RuCl₂·6H₂O (1070.960): C 53.83, H 4.71, N 10.46; found: C 54.17, H 4.42, N 13.17.

2.3.3. Synthesis of RuB, RuC, RuD

The synthesis methods of RuB, RuC and RuD were similar to the RuA.

Compound RuB has been fully characterized and the results were shown in our previous report [42]. Compound RuC ¹H NMR (400 MHz, DMSO) δ (ppm): δ 9.29 (s, 2H), 8.90 (dd, *J* = 15.7, 8.2 Hz, 5H), 8.52 (d, *J* = 7.3 Hz, 2H), 8.22 (td, *J* = 8.0, 1.3 Hz, 3H), 8.11 (td, *J* = 8.0, 1.3 Hz, 3H), 7.95 (d, *J* = 4.8 Hz, 2H), 7.85 (dd, *J* = 9.4, 5.4 Hz, 5H), 7.66–7.51 (m, 8H), 7.47 (t, *J* = 7.3 Hz, 1H), 7.40–7.32 (m, 2H), 7.20–7.11 (m, 1H),

6.79–6.72 (m, 1H). Compound RuD ¹H NMR (400 MHz, DMSO) δ (ppm): δ 9.29 (s, 2H), 8.90 (dd, $J = 15.6, 8.2$ Hz, 5H), 8.22 (t, $J = 7.3$ Hz, 3H), 8.11 (t, $J = 7.2$ Hz, 5H), 7.94 (s, 2H), 7.87 (d, $J = 4.8$ Hz, 5H), 7.60 (d, $J = 12.5$ Hz, 5H), 7.45 (s, 1H), 7.36 (t, $J = 6.7$ Hz, 3H), 7.16 (s, 1H), 7.02 (d, $J = 6.4$ Hz, 1H), 6.76 (d, $J = 8.5$ Hz, 1H), 3.91 (s, 4H).

2.4. Solution preparation and metal ion titration

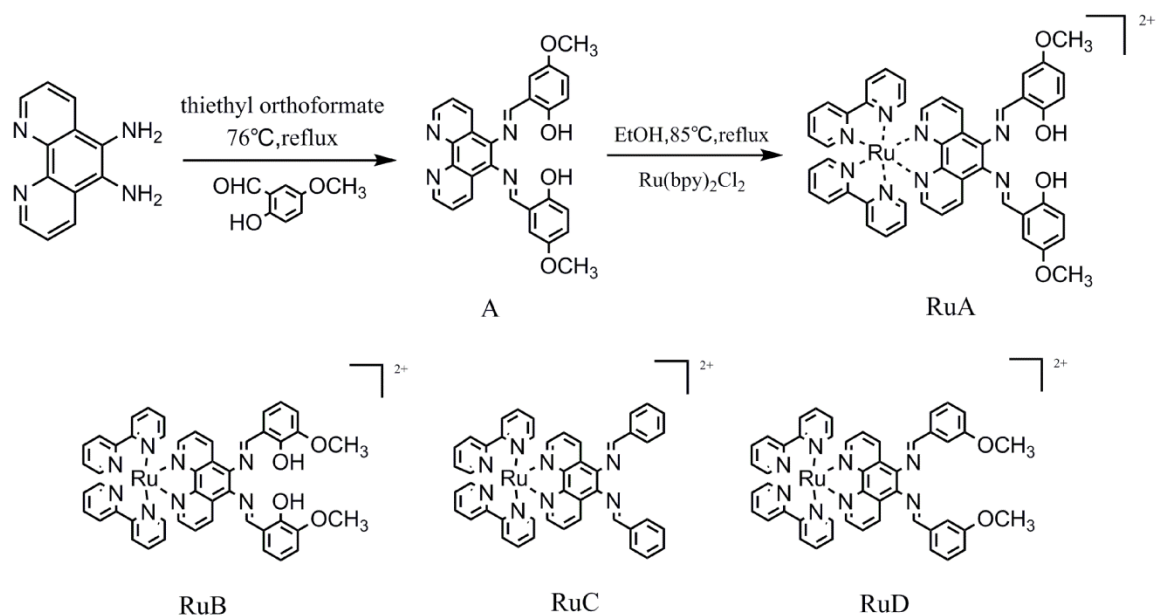
RuA stock solution (0.5 mM) was prepared in HEPES buffer (10 mM, pH=7.4) and further diluted to 15 μ M for the assay. Stock solutions of various metal ions of nitrate salts (Cu^{2+} , Pb^{2+} , Na^+ , Co^{2+} , Fe^{3+} , K^+ , Ba^{2+} , Al^{3+} , Cr^{3+} , Ca^{2+} , Mg^{2+} , Ag^+ , Fe^{2+} , Cd^{2+} , Mn^{2+} , Ni^{2+} and Li^+), amino acids (L-histidine, L-cysteine, glutathione, L-methionine, L-threonine, L-glutamic acid, L-leucine, L-isoleucine, L-aspartic acid, L-arginine, L-proline, L-proline, L-serine, L-tryptophan, L-lysine, D-phenylalanine, DL-alanine and glycine) with the concentration of 15 mM were prepared in distilled water and then diluted to appropriate concentrations. NEM (60 mM) stock solution was prepared in distilled water and kept at 4 °C before used. RuA (1.00 mL, 15 μ M) and suitable amounts of ions solution were added into the cuvette. As for the selective and competitive detection of various metal cations and luminescence titration of Cu^{2+} , the luminescence spectra were recorded after incubation for 1 min at room temperature. Similarly, the incubation time was 4 min for the detection of L-His. All the luminescence spectra were collected under excitation at 460 nm. Slit: 10/10 nm.

2.5. Cell culture and cell imaging

Mice B16 melanoma cells were cultured in 1640 Medium with 1% antibiotics (penicillin-streptomycin, 10 kU mL⁻¹) and 10% FBS (fetal bovine serum) under a 5% CO₂ humid atmosphere (37 °C). Firstly, the cells were seeded into a 48-well plate and incubated for 24 h. Then the cells were washed three times with phosphate buffered saline (PBS, pH=7.4). Next, after incubating with 30 μ M RuA for 2 h, the cells were washed thrice again with PBS to remove the free RuA. Then 1640 culture medium (1 mL) was added and the cellular uptake was observed by confocal laser scanning microscopy

with 460 nm as excitation wavelength. For the second experiment, cells were pre-incubated with N-ethylmaleimide (400 μM) for 15 min and washed with PBS three times, then the cells were treated with RuA (30 μM) for 2 h, and then treated with Cu^{2+} (40 μM). For the third experiment, cells were pre-incubated with N-ethylmaleimide (400 μM) for 15 min, and then treated with RuA (30 μM), Cu^{2+} (40 μM) for 2 h. Prior to imaging, cells were incubated with L-His (100 μM).

3. Results and Discussion



Scheme 1. The synthesis of RuA and the structure of RuB, RuC and RuD.

3.1. Optical properties of RuA

The optical properties of probe RuA were studied by UV-Vis absorption and luminescence spectroscopy. As shown in Figure 1A, the UV-Vis absorption spectrum of RuA showed a typical absorption peak around 290 nm due to the $\pi-\pi^*$ transition of 2,2'-bipyridine moieties; the peaks at 340 nm and 460 nm were ascribed to the charge transfer (CT) transition of phenanthroline-based units (Schiff base cavity) and a metal to ligand charge transfer (MLCT) absorption band, respectively [34,43]. Moreover, it can be seen that RuA exhibited the maximum emission at 604 nm and the maximum excitation at 460 nm, and no excitation dependence was observed (Fig. 1B). Therefore, in the

following experiments, the excitation wavelength of probe RuA was fixed at 460 nm, which corresponded to the UV-Vis peak of MLCT.

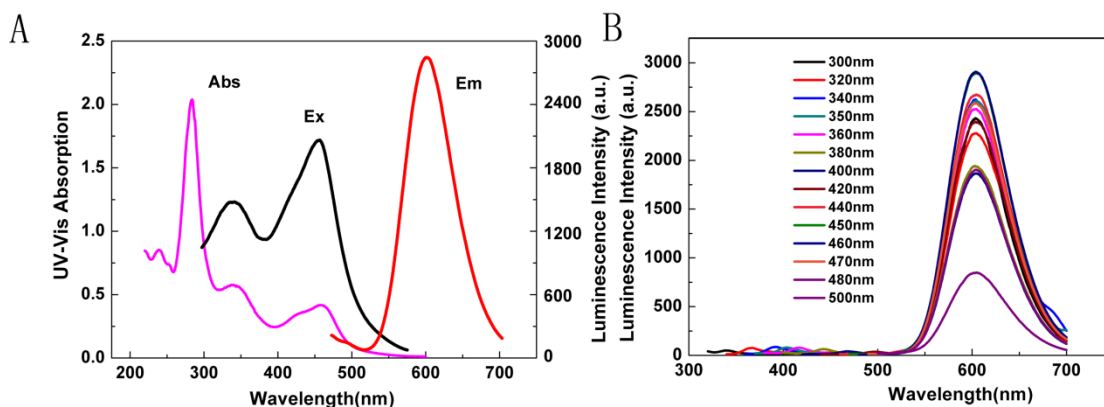


Fig. 1. (A) The UV-Vis absorption spectrum, excitation and emission luminescence spectra of RuA (15 μM). (B) Luminescence emission spectra of RuA (15 μM) at the different excitation wavelength. All spectra were measured in HEPES buffer (10 mM, pH=7.4).

3.2. Investigation of the analytical conditions

At first, we studied the effect of the concentration of probe RuA. As shown in Fig. 2A, when the concentration of RuA was more than 12 μM , the quenching efficiency ($(I_0-I)/I_0$) changed moderately by adding the same concentration of Cu^{2+} into the solution. Considering the gain of low detection limit and good luminescence spectrum, 15 μM was served as the appropriate concentration of RuA in this experiment. pH was another vital factor to affect the luminescent detecting performance. So the effect of pH towards the luminescence quenching efficiency of RuA was also investigated in the solution of Cu^{2+} (15 μM) and RuA (15 μM). The result as shown in Fig. 2B illustrated that a high quenching efficiency could be obtained at pH=7.2-9.0. This can be attributed to that the deprotonation of phenolic hydroxyl in mildly basic condition would induce the oxygen atom and nitrogen atom to bind to Cu^{2+} better [44]. Considering that the normal physiological conditions is pH=7.4, therefore, this value was selected as the operating pH condition in our experiment. Furthermore, the influence of reaction time was shown in

Fig. S1A. It can be seen that the luminescence intensity of RuA decreased by 90% in less than 1 min with the addition of Cu^{2+} , revealing a fast reaction rate. However, the luminescence intensity increased gradually and achieved a stable state after 4 min when L-His was added into the RuA–Cu(II) solution (Fig. S1B†). Therefore, the reaction time of 1 min and 4 min were selected for the detection of Cu^{2+} and L-His, respectively. Additionally, the stability of RuA-Cu (II) and RuA-Cu (II) + L-His was investigated in different concentrations of NaCl solution, and only mild luminescence intensity changes can be observed even at the high ionic strength condition (Fig. 2C). The photostability of RuA was also studied, and the luminous intensity remained almost constant under 2 h continuous irradiation (460 nm) with a Xe lamp (Fig. 2D). Based on above results, the probe can be applied to biologic imaging and biomarkers.

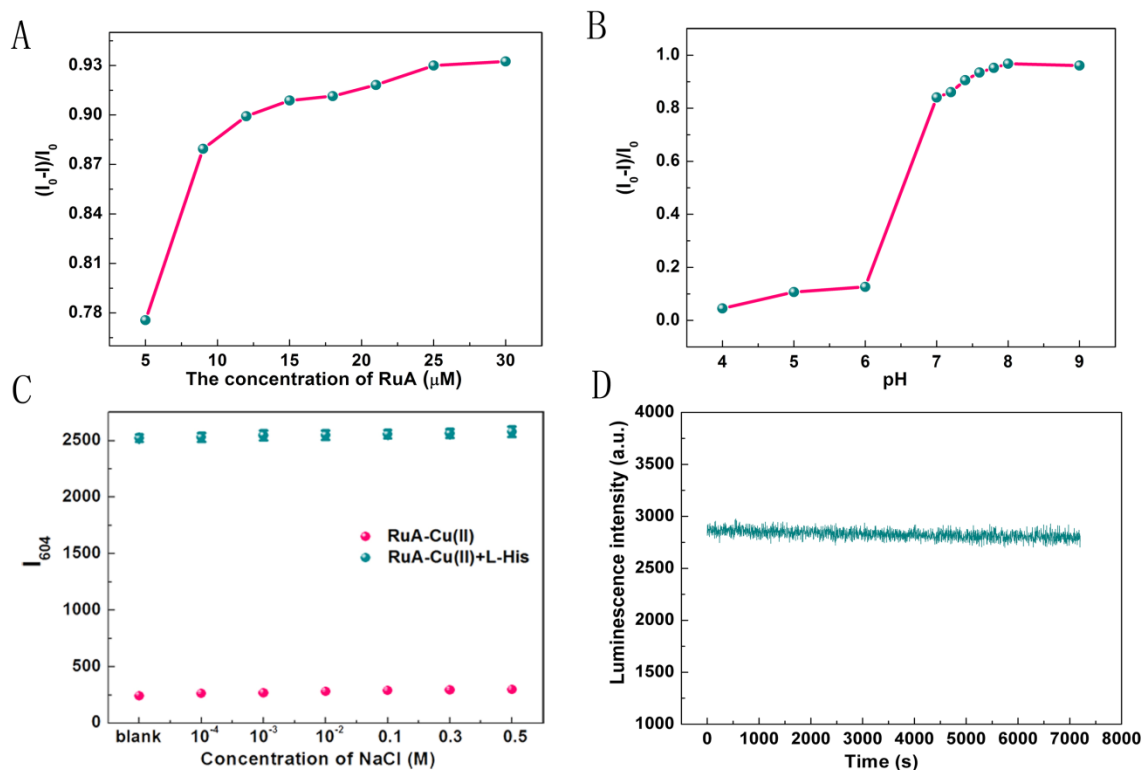


Fig. 2. (A) The effect of concentration of RuA on the luminescence quenching efficiency. (B) The effect of pH on the luminescence quenching efficiency of RuA. (C) Luminescence intensity of RuA-Cu(II) (15 μM) and RuA-Cu(II) (15 μM) + L-His (30

μM) containing different concentrations of NaCl (error bars, SD, $n=3$). (D) The photostability of RuA (15 μM) under continuous UV irradiation. The excitation/emission wavelengths were 460/604 nm. All spectra were tested in HEPES buffer (10 mM, pH=7.4).

3.3. Detection of Cu^{2+}

The selectivity of RuA for Cu^{2+} sensing was evaluated by adding various metal ions with a certain concentration. As shown in Fig. 3A and Fig. S2, other metal cations (Pb^{2+} , Na^+ , Co^{2+} , Fe^{3+} , K^+ , Ba^{2+} , Al^{3+} , Cr^{3+} , Ca^{2+} , Mg^{2+} , Ag^+ , Fe^{2+} , Cd^{2+} , Mn^{2+} , Ni^{2+} and Li^+) marginally affected the luminescence intensity of RuA, while Zn^{2+} caused a slight luminescence quenching. This may be ascribed to the chelation effect between RuA and Zn^{2+} , which can lead to the electron transfer and the change in the order of energy levels of the excited states [45]. Besides, other divalent transition metal ions including Fe^{2+} , Ni^{2+} performed nearly no effect on the luminescence of RuA. Thus, the probe RuA showed high selectivity for Cu^{2+} . Moreover, the binding behavior of the probe towards a variety of metal ions was studied by the UV-Vis spectra (Fig. 3B). A bathochromic shift of 23 nm was observed in RuA+ Cu^{2+} , in comparison with the RuA, while other metal ions had nearly no interference. The UV-Vis absorption titration of RuA with Cu^{2+} was also completed, and we can clearly find that the peak at 340 nm moved slowly toward the long wavelength direction with the increase of Cu^{2+} (Fig. S3†). This was due to the coordination of the Cu^{2+} to the phenol oxygen atom and imino nitrogen atom in Schiff base cavity, which reduced the ability of the imino group to participate in the charge transfer (CT) transition [46]. These results indicated that RuA possessed a strong binding with Cu^{2+} and therefore, can be applied to detect Cu^{2+} quickly, selectively and sensitively in aqueous solution.

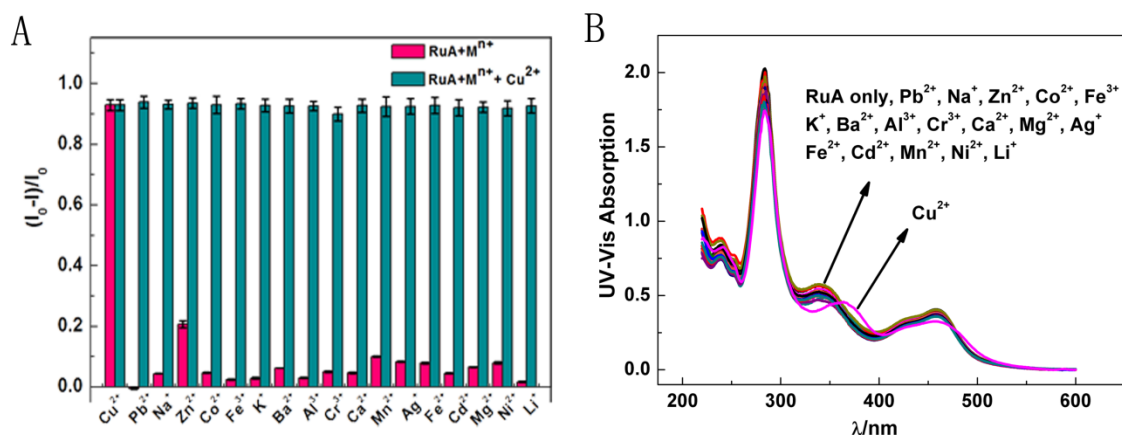


Fig. 3. (A) Selectivity of the RuA (15 μM) sensing system for Cu^{2+} (15 μM) to other competing metal ions (15 μM) (error bars, SD, $n=3$), where I_0 and I refer to the luminescence intensities of the system ($\lambda_{\text{em}}=604$ nm) in the absence and presence of metal ions, respectively. (B) Absorption spectra of RuA (15 μM) upon addition of different metal ions (15 μM). All spectra were detected in HEPES buffer (10 mM, $\text{pH}=7.4$).

The linear range and detection limit of Cu^{2+} detection was assessed by changing the concentration of Cu^{2+} at the best condition discussed above. The luminescence of RuA was quenched gradually by adding Cu^{2+} (Fig. 4A). The corresponding detection limit and linear range have been calculated to be 0.35 nM ($S/N=3$) limited from 5 nM to 9.0 μM (Fig. 4B), which is superior to the other organic probes reported previously (Table S1[†]). Besides, the Job's plot for the binding activity of RuA to Cu^{2+} was researched according to the luminescence titration (Fig. 4C), and a 1:1 stoichiometry was obtained. Furthermore, the association constant (K) was calculated to be $4.437 \times 10^3 \text{ M}^{-1}$ based on the Benesi-Hildebrand plot (Fig. 4D) [47].

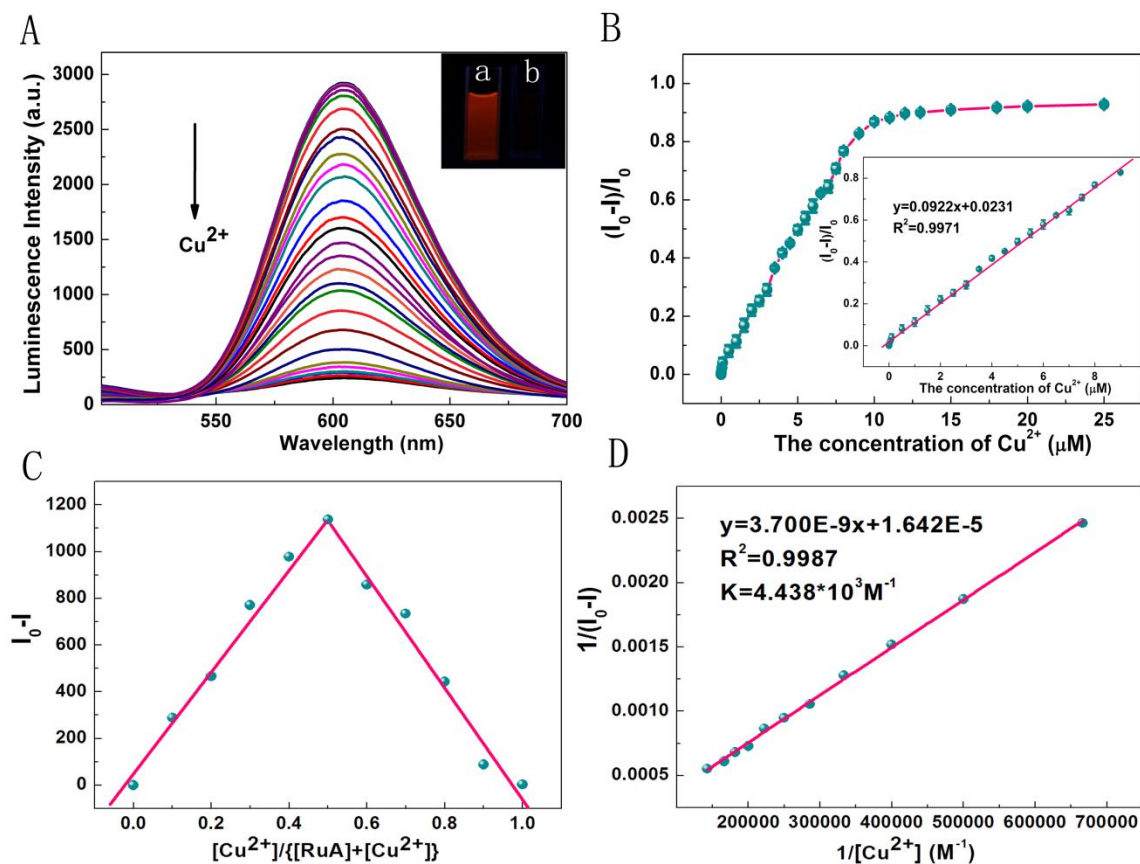


Fig. 4. (A) Luminescence emission spectra of RuA (15 μM) in the presence of different concentrations of Cu²⁺. Inset: photograph of RuA (a), and RuA+Cu²⁺ (b) under UV illumination (365 nm). (B) The plots of relative luminescence intensity $(I_0 - I)/I_0$ versus the concentration of Cu²⁺ (error bars, SD, n=3). (C) Job's plot of the complex formed by RuA and Cu²⁺ at a constant total concentration of 15 μM. (D) Benesi-Hildebrand analysis of RuA (15 μM) at different Cu²⁺ concentration. I_0 and I are the luminescence intensities of the probe at 604 nm in the absence and presence of Cu²⁺, respectively. All spectra were detected in HEPES buffer (10 mM, pH=7.4).

3.4. Detection of L-His

As expected, the RuA-Cu(II) ensemble was almost non-luminescent excited at 460 nm. However, all the L-His, cysteine (Cys) and glutathione (GSH) can induce a great increase of luminescent intensity at around 604 nm (Fig. S4[†]), which brought the interference toward L-His detection. Thus, we introduced N-ethylmaleimide (NEM) as a masking

agent to eliminate the effect of thiol groups in the detecting system [48,49] (the reaction process was shown in Scheme S2†).

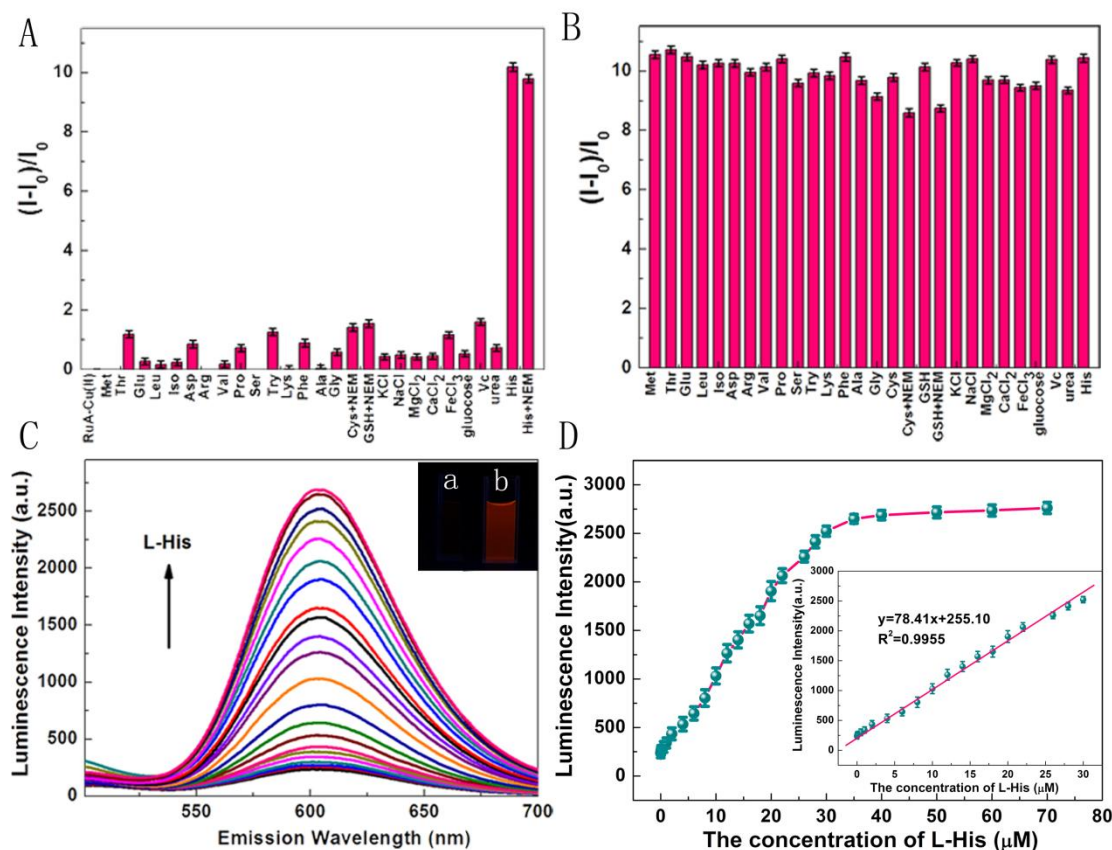


Fig. 5. (A) Luminescence responses of RuA-Cu(II) (15 μM) to amino acids (30 μM) and common biological species. (B) Luminescence responses of RuA-Cu(II) (15 μM) to L-His (30 μM) in the presence of various amino acids (30 μM) and common biological species. (C) Luminescence spectra of the RuA-Cu(II) complex (15 μM) towards various concentrations of L-His. Insert: photograph of RuA-Cu(II) complex (a), and RuA-Cu(II)+L-His (b) under UV illumination (365nm). (D) Plots of the luminescence value as a function of the L-His concentration (error bars, SD, $n=3$). All spectra were measured in HEPES buffer (10 mM, pH=7.4).

Then we inspected the selectivity of the probe towards other amino acids (30 μM) and common biological species (KCl 4 mM, NaCl 4 mM, MgCl_2 400 μM , CaCl_2 400 μM , FeCl_3 20 μM , glucose 300 μM , ascorbic acid 50 μM , urea 500 μM). As shown in Figure

5A, the luminescence of the system initiated by L-His was much more pronounced than those by other substances. We also conducted a competitive determination to further assess the selectivity, and the results showed that the probe can still particularly respond to the L-His in the presence of other related species (Fig. 5B). Therefore, the RuA-Cu(II) ensemble possessed good selectivity towards L-His and can be used as a good probe to detect L-His in biological fluids with subtle interference.

Fig. 5C showed the titration results of L-His to RuA-Cu(II) ensemble. As indicated in Fig. 5C, the luminescent intensity of RuA-Cu(II) ensemble increased significantly with adding L-His. For example, when 30 μ M of L-His was added, a 10-fold of increase of luminescence intensity was obtained compared with the original intensity. In addition, as indicated in the titration curve (Fig. 5D), the emission intensity at 604 nm increased linearly with adding L-His from 50 nM to 30 μ M ($R^2=0.9955$), and a 0.42 nM of the detection limit ($S/N=3$) can be obtained, which means that our work presented better linear range and detection limit than other previous reports (Table S2†) and have a potential to be used in practical biological fluids [50]. Furthermore, the 2: 1 binding model of L-His to Cu^{2+} has been demonstrated by Job's plot (Fig. S5A†) and a $1.025 \times 10^4 \text{ M}^{-1}$ of association constant (K) was estimated on the grounds of a Benesi-Hildebrand plot (Fig. S5B†). Moreover, Cys and GSH also displayed similar luminescence enhancement, and the detection limits were calculated to be 2.21 nM and 2.49 nM, respectively (Fig. S6† and Fig. S7†).

3.5. Mechanism for the detection of Cu^{2+} and L-His

Due to the paramagnetic nature of Cu^{2+} , the sensing mechanism of RuA for Cu^{2+} may be attributed to the luminescence quenching induced by copper-binding [51], which ultimately allows the Cu^{2+} to exhibit recognizable luminescence quenching through electron and/or energy transfer processes [52]. It is well-known that the outer layer electron configuration for Cu^{2+} is $3s^23p^63d^9$, while the electron sub-layer 3d, 4s and 4p with the relatively low level of the empty track, which can accept lone electron pair

provided by N, O atoms to form coordination compounds. Thus, the proposed specific recognition site of RuA for Cu^{2+} was Schiff base cavity composed of the phenol oxygen atom and imino nitrogen atom. Therefore, this dramatic quenching of the initial luminescence of RuA induced by Cu^{2+} is due to the reverse photoinduced electron transfer (PET) from the 2,2'-bipyridine ruthenium(II) moieties to the phenol oxygen atom and imino nitrogen atom because of the decrease in the electron density upon Cu^{2+} complexation [53,54]. Besides, in order to further prove the response mechanism of RuA, complexes of RuB, RuC and RuD were prepared, which own the similar structure as shown in Scheme 1. Specially, the position of the amino and hydroxyl groups of the RuB complex is consistent with the RuA, and it should also respond to the Cu^{2+} . However, the methoxy group in the RuB complex is designed to be located next to the hydroxyl group so as to explore the steric hindrance in the process of the combination of L-His and Cu^{2+} . In addition, for the purpose of further investigating the role of O atom in the binding of N, O hole in Schiff base with Cu^{2+} , no hydroxyl exists in the complexes of RuC and RuD, which should be no response to copper ions. Besides, we also explored the selectivity of RuB, RuC and RuD toward different metal ions (Fig. S8†, Fig. S9† and Fig. S10†). Then the responses about these four complexes toward Cu^{2+} were compared in Fig. 6A. As expected, RuB showed an obvious luminescence quenching toward Cu^{2+} , while RuC and RuD exhibited marginal change. The reason may be that both the phenolic hydroxyls and imino group exist in RuB and the location is adjacent to each other, while no phenolic hydroxyls exists in RuC and RuD. These results demonstrated that the adjacent oxygen atom plays an indispensable role in the Cu^{2+} coordination. It is well known, the general coordination number of Cu^{2+} is four, so the adjacent amido and hydroxyl of the probe provide four coordination groups to combine with Cu^{2+} to form a complex. Moreover, we noticed that the luminescence can be enhanced by introducing L-His into the RuA-Cu(II) and RuB-Cu(II) systems (Fig. 6B), implying that the strong binding capacity of the imidazole group from L-His with Cu^{2+} and freeing Ru(II) compounds from the

complexes and thus recovering their luminescence [55]. However, RuA had better luminescence recovery than RuB, thus RuA was selected as the representative probe in this work.

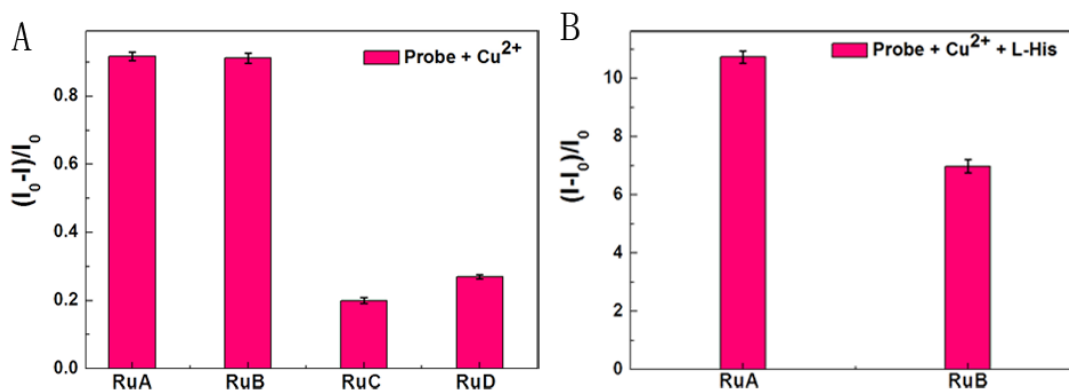


Fig. 6. The luminescence response of Ru compounds (15 μM) toward Cu^{2+} (15 μM) (A) and L-His (30 μM) (B) in HEPES buffer (10 mM, pH=7.4), where I_0 and I refer to the luminescence intensities of the system ($\lambda_{\text{em}}=604$ nm) in the absence and presence of Cu^{2+} or L-His, respectively.

Above hypothesis also has been confirmed by MALDI-TOF-MS spectrum of RuA solution in the presence of Cu^{2+} from Fig. 7A, which two peaks related to RuA-Cu(II) ensemble have been observed. Then the ESI-MS spectra of RuA+Cu(II)+L-His solution were also obtained (Fig. 7B), in which the peaks at $m/z \sim 890.33$ and 984.17 were related to RuA, and the appearance of a peak at 374.10 evidenced the formation of the complex $[\text{2L-His} + \text{Cu}^{2+}]$. Additionally, ^1H NMR titration of the RuA can further support the proposed mechanism (Fig. 7C). It can be seen from Fig. 7C that the peaks about RuA in the ^1H NMR spectrum were broadened and even almost vanished when the Cu^{2+} was added, which may be due to the coordination of paramagnetic Cu^{2+} and RuA [56]. And the addition of L-His into the RuA-Cu (II) solution resulted in a recovery of the fine ^1H NMR spectrum of RuA in the mixture to some extent, which indicated that L-His was able to remove Cu^{2+} from the RuA-Cu (II) complex. What's more, the displacement mechanism was further testified by UV spectra, in which the formation of free RuA was

clearly observed when adding L-His into RuA–Cu(II) solution (Fig. S11†). The quantum yield of RuA and RuA-Cu(II)+L-His were 0.084 and 0.081, respectively (reference was fluorescein in 0.1 N NaOH, $\Phi = 0.85$) (Fig. S12†) [57]. Besides, a luminescence decay experiment was also conducted, and the lifetimes of RuA, RuA-Cu(II) and RuA-Cu(II)+L-His were determined to be 258.7, 108.8 and 250.8 ns, respectively, by fitting the data into a single exponential decay function (Fig. S13†). These results were all consistent with the proposed mechanism, as indicated in Scheme 2.

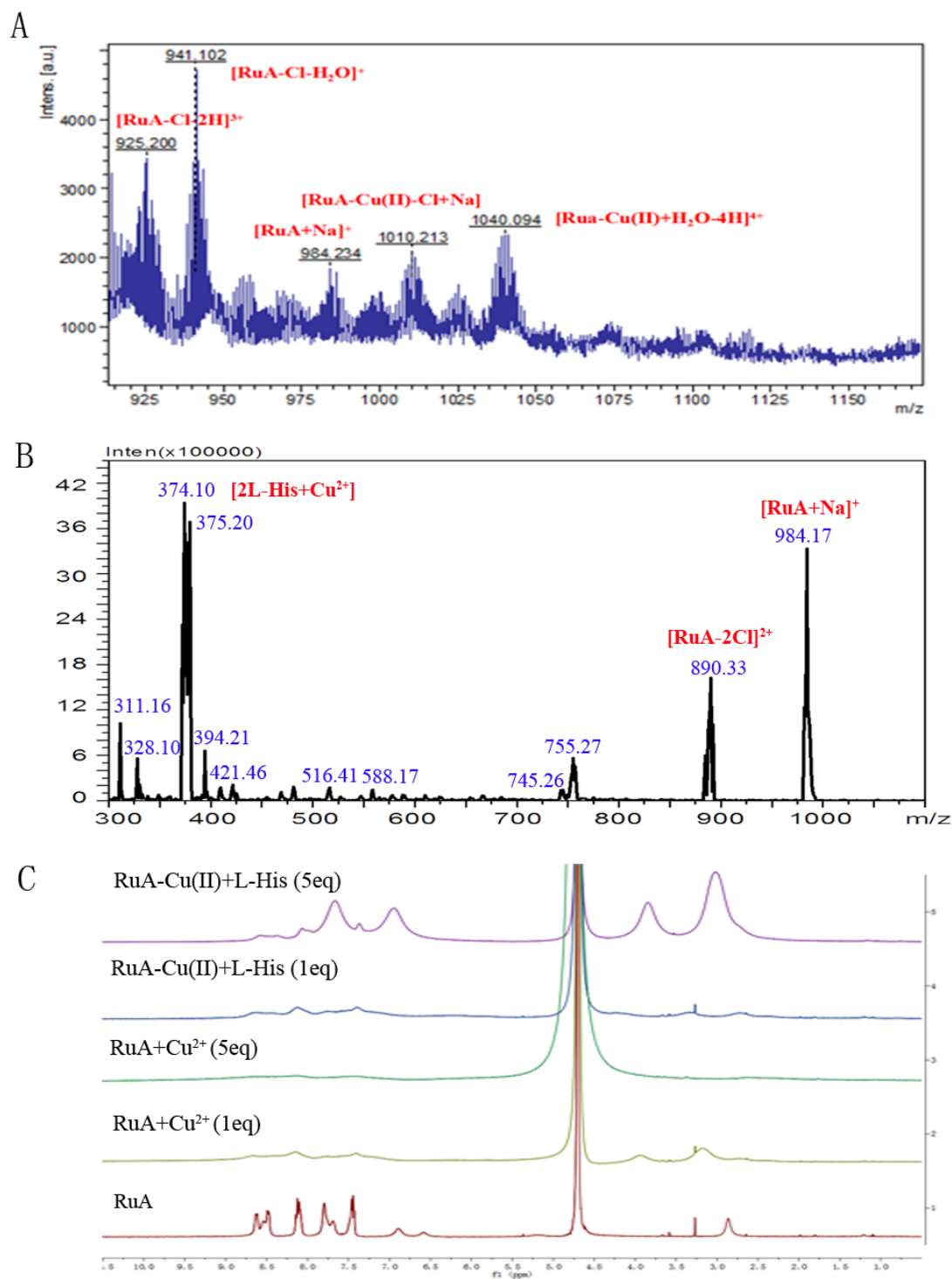
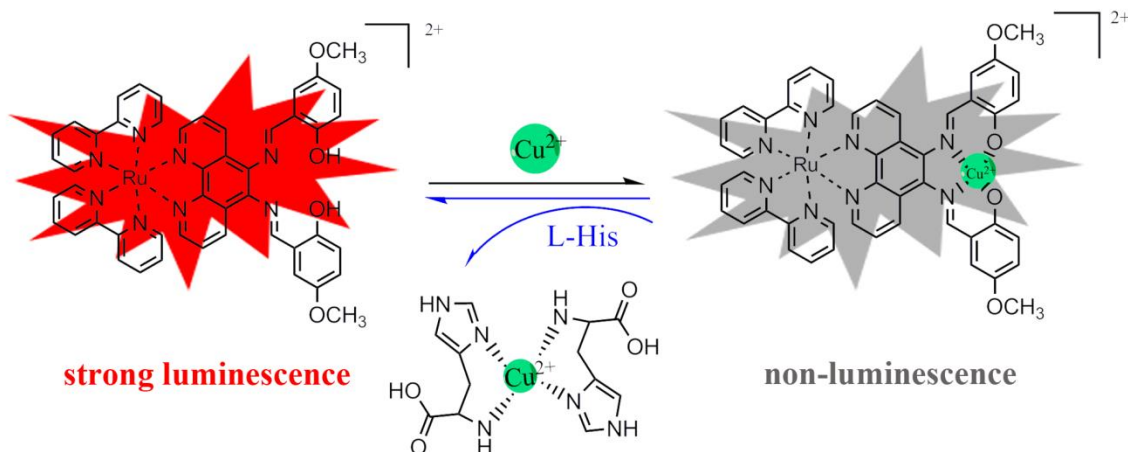


Fig. 7. (A) MALDI-TOF-MS of $\text{RuA}+\text{Cu}^{2+}$ in methanol. (B) ESI-MS spectrum of $\text{RuA}-\text{Cu}(\text{II})+\text{L}-\text{His}$ in HEPES buffer solution. (C) ^1H NMR titration spectrum of RuA with Cu^{2+} followed by $\text{L}-\text{Histidine}$ in D_2O .



Scheme 2. The proposed mechanism of Cu^{2+} and L-His detection.

3.6. Real sample analysis

3.6.1. Cu^{2+} detection in water samples

According to the water quality standard of US Environmental Protection Agency (EPA), $20 \mu\text{M}$ is the highest acceptable level of Cu^{2+} in drinking water [58]. RuA probe was water-soluble with the luminescent detection limit of 0.35 nM and this suggested that it can be applied to detecting Cu^{2+} in drinking water samples. In fact, the good results have been gained from the detection of Cu^{2+} in tap water (Table S3).

3.6.2. L-Histidine detection in biological fluids

Since L-His is an essential component of many proteins and associated with various diseases, it is important to detect L-His in biological fluids such as human serum and urine. Before the detection, the blood and urine samples were treated according to the method described in the supporting information. In order to evaluate the accuracy of the proposed method, the spiked recovery test of L-His in the actual samples was carried out. The determination of L-His for blood samples was shown in Table S4. The original content of L-His in human serum was in the range of $15\text{--}75 \mu\text{M}$ [50]. And the average contents of L-His in two urine samples were measured to be 470 and $543 \mu\text{M}$, respectively (Table S5), which were included in the normal level ($130\text{--}2100 \mu\text{M}$) [59]. All of these results manifested that the proposed method for sensing L-His in biological fluids was accurate and reliable.

3.7. Application of probe in living cellular imaging

It is widely known that bioimaging probes for analytical diagnostics in vitro should be non-toxic. Actually, because of much smaller scattering, lower background signals and almost no damage to viable cells, the emission spectrum of the red or near-infrared (NIR) region are favorable for their use as biological probes in biological samples [60,61]. To further explore the potential applications of the RuA in the biological system, the cytotoxicity of RuA towards mice B16 melanoma cells was firstly assessed by CCK-8 assay after a 24 h treatment (Fig. S14[†]). The percentage of cell survival was more than 97%, which revealed that the RuA was non-cytotoxic towards B16 cells. Subsequently, luminescence imaging experiments of RuA for living cells were performed. As shown in Fig. 8, a bright red luminescence was observed when B16 cells were treated with the RuA probe only. When cells were pre-treated with an appropriate amount of thiol-scavenger (NEM) to eliminate all free thiols present in the cells, and then incubated with RuA and Cu²⁺, the observed luminescence signal in cells was significantly reduced. However, a remarkable luminescence signal was investigated when cells were incubated with RuA, Cu²⁺ and L-His. These results indicated that the probe RuA can be used for imaging Cu²⁺ and L-His in living cells.

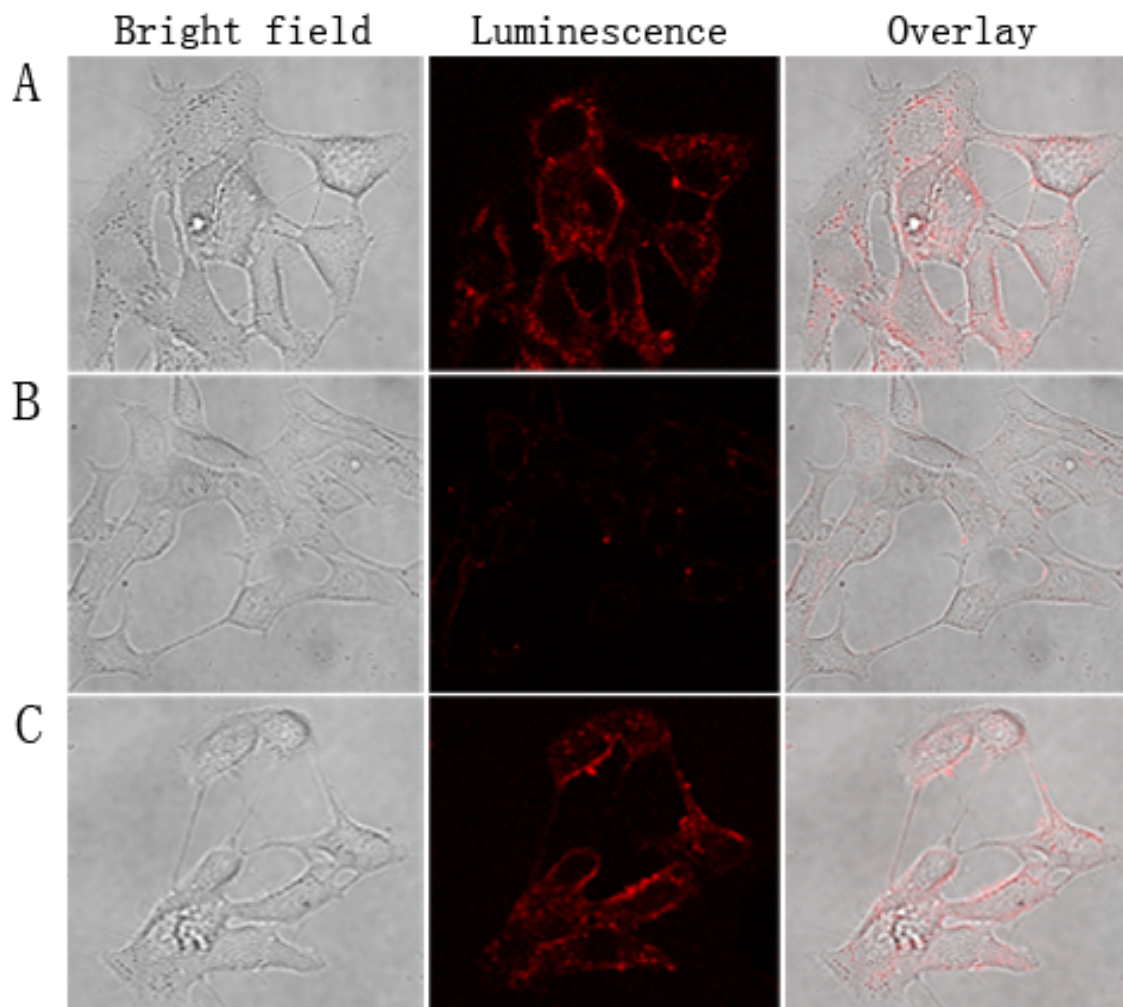


Fig. 8. Luminescence images of the living cells. (A) B16 cells were incubated with RuA (30 μM) for 2 h. Cells pre-incubated with 0.12 mM NEM for 15 min, washed thrice, treated with RuA (30 μM) for 2 h, then treated with Cu^{2+} (40 μM) (B) and then treated with L-His (100 μM) (C). Luminescence images were acquired by confocal microscopy (excitation 460 nm, emission 550–680 nm). Scale bar: 25 μm .

4. Conclusion

In summary, the water-soluble luminescent RuA was used as an on-off-on probe for sensitively and selectively detecting Cu^{2+} and L-Histidine, revealing the low detection limits of 0.35 nM and 0.44 nM for Cu^{2+} and L-Histidine, respectively. Cu^{2+} can significantly quench the luminescence of RuA by the coordination of Cu^{2+} with the N, O

atoms of the probe molecule. Furthermore, the sensing mechanism was demonstrated by luminescent behaviour of similar structure compounds (RuB, RuC and RuD) and MALDI-TOF-MS spectrum of co-existence solution of RuA and Cu^{2+} . Upon adding L-Histidine into RuA-Cu(II) solution, the luminescence can be almost recovered to the original intensity. The possible cause of the luminescence enhancement was L-Histidine being able to remove Cu^{2+} from RuA-Cu(II) due to the strong binding ability towards Cu^{2+} of the amino and imidazole group of L-Histidine and RuA released from the ensemble. In addition, this replace mechanism was also testified by MS, ^1H NMR, UV-Vis and other characterizations. Besides, the probe can practically be applied to the analysis of real samples. Importantly, the low-toxicity probe can be used for imaging Cu^{2+} and L-His in living cells. Finally, the excellent performance of the probe indicated its potential application in the field of environmental and clinical diagnostics.

Acknowledgements

We would like to thank the National Natural Science Foundation of China (Nos. 21407109) for its financial support to this research.

Appendix A. Supplementary Data

Supplementary data to this article can be found online at

Reference

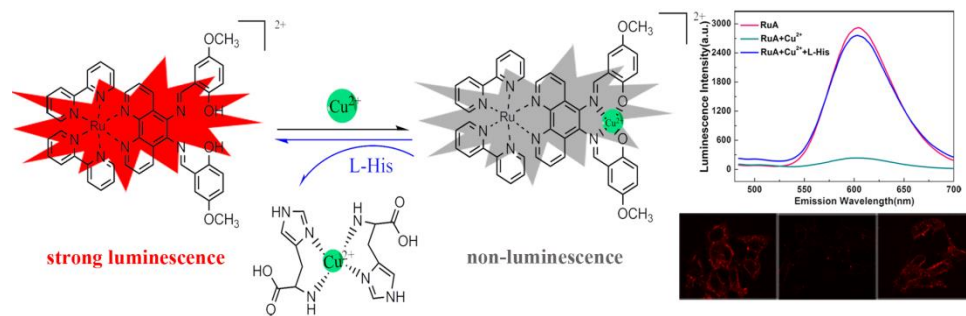
- [1] M. Debabrata, T. Govindaraju, *Chem - Eur. J.* 17 (2011) 1410-1414.
- [2] N. Narayanaswamy, T. Govindaraju, *Sens. Actuators B* 161 (2012) 304-310.
- [3] E. Gaggelli, H. Kozłowski, D. Valensin, G. Valensin, *Chem. Rev.* 37 (2006) 1995-2044.
- [4] R. Uauy, M. Olivares, M. Gonzalez, *Nutr. Rev.* 45 (1987) 176–180.
- [5] M. C. Linder, M. Hazeghazam, *Am. J. Clin. Nutr.* 63 (1996) 797S-811S.
- [6] J. S. Valentine, P. J. Hart, *P. Natl. Acad. Sci.* 100 (2003) 3617-3622.
- [7] L. I. Bruijn, T. M. Miller, D. W. Cleveland, *Annu. Rev. Neurosci.* 27(2004) 723-749.

- [8] T. Chen, Y. Hu, Y. Cen, X. Chu, Y. Lu, *J. Am. Chem. Soc.* 135 (2013) 11595-11602.
- [9] D. R. Brown, H. Kozłowski, *Dalton. T.* 13 (2004) 1907-1917.
- [10] S. G. Kaler, *Nat. Rev. Neurol.* 7 (2011) 15-29.
- [11] S. Lutsenko, A. Gupta, J. L. Burkhead, V. Zuzel, *Arch. Biochem. Biophys.* 476 (2008) 22-32.
- [12] G. L. Millhauser, *Accounts Chem. Res.* 37 (2004) 79-85.
- [13] S. V. Staden, L. Holo, *Sens. Actuators B* 120 (2007) 399-402.
- [14] L. D. Li, Z. B. Chen, H. T. Zhao, L. Guo, *Biosens. Bioelectron.* 26 (2011) 2781-2785.
- [15] W. M, S. ME, Q. AR, G.-L. E, B. P, H. O, S. P, L. B, *Am. J. Clin. Nutr.* 87 (2008) 1860-1866.
- [16] G. N. Chen, X. P. Wu, J. P. Duan, H. Q. Chen, *Talanta* 49 (1999) 319-330.
- [17] M. L. Rao, H. Stefan, C. Scheid, A. D. Kuttler, W. Froscher, *Epilepsia* 34 (1993) 347-354.
- [18] A.L. Jones, M.D. Hulett, C.R. Parish, *Immunol. Cell. Biol.* 83 (2005) 106-118.
- [19] E.L. Que, D.W. Domaille, C.J. Chang, *Chem. Rev.* 39 (2008) 1517-1549.
- [20] X. Chen, T. Pradhan, F. Wang, J.S. Kim, J. Yoon, *Chem. Rev.* 112 (2012) 1910-1956.
- [21] J. Du, M. Hu, J. Fan, X. Peng, *Chem. Soc. Rev.* 43 (2012) 4511-4535.
- [22] L. Prodi, F. Bolletta, M. Montalti, N. Zaccheroni, *Coordin. Chem. Rev.* 205 (2000) 59-83.
- [23] C. Bargossi, M.C. Fiorini, M. Montalti, L. Prodi, N. Zaccheroni, *Cheminform* 208 (2000) 17-32.
- [24] Z. Huang, J. Du, J. Zhang, X.Q. Yu, L. Pu, *Chem. Commun.* 48 (2012) 3412-3414.
- [25] F. Pu, Z. Huang, J. Ren, X. Qu, *Anal. Chem.* 82 (2010) 8211-8216.
- [26] S. K. Sun, K. X. Tu, X. P. Yan, *Analyst* 137 (2012) 2124-2128.
- [27] P. N. Basa, A. G. Sykes, *J. Org. Chem.* 77 (2012) 8428-8434.

- [28] X. Li, Y. Chen, J. Meng, K. Lü, A. Zhang, B. Zhang, *Chinese J. Chem.* 29 (2011) 1947-1950.
- [29] J. Xie, M. Ménand, S. Maisonneuve, R. Métivier, *J. Org. Chem.* 72 (2007) 5980-5985.
- [30] B. Khan, M.R. Shah, D. Ahmed, M. Rabnawaz, I. Anis, S. Afridi, T. Makhmoor, M.N. Tahir, *J. Hazard. Mater.* 309 (2016) 97-106.
- [31] M.H. Kim, H.H. Jang, S. Yi, S.K. Chang, M.S. Han, *Chem. Commun.* 32 (2009) 4838-4840.
- [32] N. Li, Y. Xiang, A. Tong, *Chem. Commun.* 46 (2010) 3363-3365.
- [33] V. Balzani, G. Bergamini, F. Marchioni, P. Ceroni, *Coord. Chem. Rev.* 250 (2006) 1254-1266.
- [34] M. Hardy, D. Konetski, C. Bowman, N. Devaraj, *Org. Biomol. Chem.* 14 (2016) 5555-5558.
- [35] P. Zhou, Z. Zheng, W. Lu, F. Zhang, Z. Zhang, D. Pang, B. Hu, Z. He, H. Wang, *Angew. Chem. Int. Edit.* 51 (2012) 670-674.
- [36] Y. Yang, Q. Zhao, W. Feng, F. Li, *Chem. Rev.* 113 (2013) 192-270.
- [37] N. P. Cook, K. Kilpatrick, L. Segatori, A. A. Martí, *J. Am. Chem. Soc.* 134 (2012) 20776-20782.
- [38] H. Komatsu, K. Yoshihara, H. Yamada, Y. Kimura, A. Son, K. Tanabe, *Chem - Eur. J.* 19 (2013) 1971-1977.
- [39] W. Hao, A. McBride, S. McBride, P. G. Jian, Y. W. Zhi, *J. Mater. Chem.* 21 (2010) 1040-1048.
- [40] M. Suresh, A. Ghosh, A. Das, *Chem. Commun.* 2008 (2008) 3906-3908.
- [41] G. U. Reddy, P. Das, S. Saha, M. Baidya, S. K. Ghosh, A. Das, *Chem. Commun.* 49 (2013) 255-257.
- [42] P. P. Li, Z. Y. Jin, M. L. Zhao, Y. X. Xu, Y. Guo, D. Xiao, *Dalton T.* 44 (2015) 2208-2216.

- [43] R. Lo, S. Roy, T. Banerjee, B. Ganguly, A. Das, *Chem. Commun.* 49 (2013) 9818-9820.
- [44] T. Chen, L. Yin, C. Huang, Y. Qin, W. Zhu, Y. Xu, X. Qian, *Biosens. Bioelectron.* 66 (2015) 259-265.
- [45] T. Kowalczyk, Z. Lin, T.V. Voorhis, *J. Phys. Chem. A* 114 (2010) 10427-10434.
- [46] T. Gunnlaugsson, J. P. Leonard, N. S. Murray, *Org. Lett.* 6 (2004) 1557-1560.
- [47] M. Hariharan, S. C. K. And, D. Ramaiah, *Org. Lett.* 9 (2007) 417-420.
- [48] H. S. Jung, J. H. Han, Y. Habata, C. Kang, J.S. Kim, *Chem. Commun.* 47 (2011) 5142-5144.
- [49] H. Li, J. Liu, Y. Fang, Y. Qin, S. Xu, Y. Liu, E. Wang, *Biosens. Bioelectron.* 41 (2013) 563-568.
- [50] H. Agarwalla, N. Taye, S. Ghorai, S. Chattopadhyay, A. Das, *Chem. Commun.* 50 (2014) 9899-9902.
- [51] Z. Zheng, L. Wang, W. Tang, P. Chen, H. Zhu, Y. Yuan, G. Li, H. Zhang, G. Liang, *Biosens. Bioelectron.* 83 (2016) 200-204.
- [52] S. Anbu, S. Shanmugaraju, R. Ravishankaran, A.A. Karande, P.S. Mukherjee, *Inorg. Chem. Commun.* 25 (2012) 26-29.
- [53] S. Anbu, S. Shanmugaraju, R. Ravishankaran, A.A. Karande, P.S. Mukherjee, *Dalton T.* 41 (2012) 13330-13337.
- [54] S. Anbu, R. Ravishankaran, G.D.S. Mf, A.A. Karande, A.J. Pombeiro, *Inorg. Chem.* 53 (2014) 6655-6664.
- [55] F. Pu, Z. Huang, J. Ren, X. Qu, *Anal. Chem.* 82 (2010) 8211-8216.
- [56] L. Xu, Y. Xu, W. Zhu, B. Zeng, C. Yang, B. Wu, X. Qian, *Org. Biomol. Chem.* 9 (2011) 8284-8287.
- [57] T. Miura, Y. Urano, K. Tanaka, T. Nagano, K. Ohkubo, S. Fukuzumi, *J. Am. Chem. Soc.* 125 (2003) 8666-8671.

- [58] H. S. Jung, P. S. Kwon, J. W. Lee, J. I. Kim, C. S. Hong, J. W. Kim, S. Yan, J. Y. Lee, J. H. Lee, T. Joo, *J. Am. Chem. Soc.* 131 (2009) 2008-2012.
- [59] P. M. Kovach, *M. E. Anal. Chem.* 54 (1982) 217-220.
- [60] B. Tang, H. Huang, K. Xu, L. Tong, G. Yang, X. Liu, L. An, *Chem. Commun.* 0 (2006) 3609-3611.
- [61] M. Li, X. Wu, Y. Wang, Y. Li, W. Zhu, T.D. James, *Chem. Commun.* 50 (2014) 1751-1753.



Graphical abstract

Highlights

- A novel near-infrared luminescent probe for the highly sensitive detection of Cu^{2+} and L-Histidine in aqueous solution has been established.
- Low detection limits and favorable linear ranges for Cu^{2+} and L-Histidine were obtained.
- The mechanism for detecting Cu^{2+} and L-Histidine has been comprehensively and clearly proposed via various methods like MS, ^1H NMR, UV-Vis etc.
- The probe that exhibited many satisfied properties has been successfully adopted to many practical applications including imaging cancer cells.